

On the Discrepancy of pp , $\bar{p}p$ Total Cross Sections at $\sqrt{s} = 1.8\text{TeV}$ between E710, E811 and CDF

Keiji IGI and Muneyuki ISHIDA^a

Theoretical Physics Laboratory, RIKEN, Wako, Saitama 351-0198, Japan

^a*Department of Physics, School of Science and Engineering, Meisei University, Hino, Tokyo 191-8506, Japan*

Based on the previous approach, we have investigated a possibility to resolve the discrepancy between the E710, E811 and CDF at $\sqrt{s} = 1.8\text{TeV}$, using the experimental data of the pp , $\bar{p}p$ total cross sections $\sigma_{\text{tot}}^{(+)}$ and $\rho^{(+)}$ ratio up to the SPS experiments ($\sqrt{s} = 0.9\text{TeV}$) as inputs. We predict $\sigma_{\text{tot}}^{\bar{p}p}$ and $\rho^{\bar{p}p}$ at the Tevatron energy ($\sqrt{s} = 1.8\text{TeV}$) as $\sigma_{\text{tot}}^{\bar{p}p} = 75.9 \pm 1.0\text{mb}$, $\rho^{\bar{p}p} = 0.136 \pm 0.005$.

It turns out that only the data of E710 is consistent with the prediction in the one standard deviation. So we can conclude that E710 is preferable but we can exclude neither CDF nor E811 results.

§1. Introduction

Recently,¹⁾ we have searched for the simultaneous best fit of the average of $\bar{p}p$, pp total cross sections($\sigma_{\text{tot}}^{(+)}$), and the ratio of the real to imaginary part of the forward scattering amplitude($\rho^{(+)}$) for $70\text{GeV} < P_{\text{lab}} < P_{\text{large}}$ as inputs in terms of high-energy parameters c_0 , c_1 , c_2 and $\beta_{P'}$ constrained by the FESR with $N(\simeq 10\text{GeV})$. Block and Halzen^{2),3)} also reached to the similar conclusions independently based on duality in a different approach. We first chose $P_{\text{large}} = 2100\text{GeV}$ corresponding to the ISR region($\sqrt{s} \simeq 60\text{GeV}$). Secondly we chose $P_{\text{large}} = 2 \times 10^6\text{GeV}$ corresponding to the Tevatron energy($\sqrt{s} \simeq 2\text{TeV}$). We then predicted $\sigma_{\text{tot}}^{(+)}$ and $\rho^{(+)}$ at the LHC and the high-energy cosmic-ray energy regions. It turned out that the prediction of $\sigma_{\text{tot}}^{(+)}$ agrees with pp experimental data at the cosmic-ray regions⁴⁾⁻⁶⁾ within errors in the first case(ISR). It has to be noted that the energy range of predicted $\sigma_{\text{tot}}^{(+)}$, $\rho^{(+)}$ is several orders of magnitude larger than the energy regions of $\sigma_{\text{tot}}^{(+)}$, $\rho^{(+)}$ input. If we use data up to Tevatron(the second case), the situation has been much improved although there are some systematic uncertainty coming from discrepancy of the data between E710,⁷⁾ E811⁸⁾ and CDF⁹⁾ at $\sqrt{s} = 1.8\text{TeV}$.¹⁾ Finally we concluded that the precise measurements of $\sigma_{\text{tot}}^{\bar{p}p}$ in the coming LHC experiments will resolve this discrepancy at $\sqrt{s} = 1.8\text{TeV}$.

The purpose of this paper is to investigate a possibility to resolve this discrepancy using the experimental data of $\sigma_{\text{tot}}^{(+)}$ and $\rho^{(+)}$ up to the SPS experiments ($\sqrt{s} = 0.9\text{TeV}$).

§2. The general approach

As in the previous paper,¹⁾ let us first consider the crossing-even forward scattering amplitude defined by

$$F^{(+)}(\nu) = \frac{f^{\bar{p}p}(\nu) + f^{pp}(\nu)}{2} \quad \text{with} \quad \text{Im } F^{(+)}(\nu) = \frac{k \sigma_{\text{tot}}^{(+)}(\nu)}{4\pi}. \quad (2.1)$$

We also assume

$$\begin{aligned} \text{Im } F^{(+)}(\nu) &= \text{Im } R(\nu) + \text{Im } F_{P'}(\nu) \\ &= \frac{\nu}{M^2} \left(c_0 + c_1 \log \frac{\nu}{M} + c_2 \log^2 \frac{\nu}{M} \right) + \frac{\beta_{P'}}{M} \left(\frac{\nu}{M} \right)^{\alpha_{P'}} \end{aligned} \quad (2.2)$$

at high energies ($\nu > N$). It is to be noted that c_0, c_1, c_2 and $\beta_{P'}$ are dimensionless. We have defined the functions $R(\nu)$ and $F_{P'}(\nu)$ by replacing μ by M in Eq. (3) of ref. 10). Here, M is the proton(anti-proton) mass and ν, k are the incident proton(anti-proton) energy, momentum in the laboratory system, respectively.

Since the amplitude is crossing-even, we have

$$\begin{aligned} R(\nu) &= \frac{i\nu}{2M^2} \left\{ 2c_0 + c_2\pi^2 + c_1 \left(\log \frac{e^{-i\pi}\nu}{M} + \log \frac{\nu}{M} \right) \right. \\ &\quad \left. + c_2 \left(\log^2 \frac{e^{-i\pi}\nu}{M} + \log^2 \frac{\nu}{M} \right) \right\}, \end{aligned} \quad (2.3)$$

$$F_{P'}(\nu) = -\frac{\beta_{P'}}{M} \left(\frac{(e^{-i\pi}\nu/M)^{\alpha_{P'}} + (\nu/M)^{\alpha_{P'}}}{\sin \pi \alpha_{P'}} \right), \quad (2.4)$$

and subsequently obtain

$$\text{Re } R(\nu) = \frac{\pi\nu}{2M^2} \left(c_1 + 2c_2 \log \frac{\nu}{M} \right), \quad (2.5)$$

$$\text{Re } F_{P'}(\nu) = -\frac{\beta_{P'}}{M} \left(\frac{\nu}{M} \right)^{0.5}, \quad (2.6)$$

substituting $\alpha_{P'} = \frac{1}{2}$ in Eq. (2.4).

FESR: The FESR corresponding to $n = 1^{(11), (12)}$ is:

$$\begin{aligned} &\int_0^M \nu \text{Im } F^{(+)}(\nu) d\nu + \frac{1}{4\pi} \int_0^{\bar{N}} k^2 \sigma_{\text{tot}}^{(+)}(k) dk \\ &= \int_0^N \nu \text{Im } R(\nu) d\nu + \int_0^N \nu \text{Im } F_{P'}(\nu) d\nu \quad . \end{aligned} \quad (2.7)$$

We call Eq. (2.7) as the FESR which we use in our analysis.

The $\rho^{(+)}$ ratio: The $\rho^{(+)}$ ratio, the ratio of the real to imaginary part of $F^{(+)}(\nu)$ was obtained from Eqs. (2.2), (2.5) and (2.6) as

$$\rho^{(+)}(\nu) = \frac{\text{Re } F^{(+)}(\nu)}{\text{Im } F^{(+)}(\nu)} = \frac{\text{Re } R(\nu) + \text{Re } F_{P'}(\nu)}{\text{Im } R(\nu) + \text{Im } F_{P'}(\nu)}$$

$$= \frac{\frac{\pi\nu}{2M^2} (c_1 + 2c_2 \log \frac{\nu}{M}) - \frac{\beta_{P'}}{M} \left(\frac{\nu}{M}\right)^{0.5}}{\frac{k\sigma_{\text{tot}}^{(+)}(\nu)}{4\pi}}. \quad (2.8)$$

Although the numerator of Eq. (2.8) becomes large for large values of ν , a real constant has to be introduced in principle since the dispersion relation for $\text{Re } F^{(+)}(\nu)$ requires a single subtraction constant $F^{(+)}(0)$.^{2),13)} So, we also add $F^{(+)}(0)$ in the numerator as

$$\rho^{(+)}(\nu) = \frac{\frac{\pi\nu}{2M^2} (c_1 + 2c_2 \log \frac{\nu}{M}) - \frac{\beta_{P'}}{M} \left(\frac{\nu}{M}\right)^{0.5} + F^{(+)}(0)}{\frac{k\sigma_{\text{tot}}^{(+)}(\nu)}{4\pi}}. \quad (2.9)$$

As will be discussed in the Appendix, the introduction of this constant slightly modifies the value of $\rho^{(+)}(\nu)$ although it will not affect the value of $\sigma_{\text{tot}}^{(+)}$. So, we use the Eq. (2.9) as the value of $\rho^{(+)}(\nu)$ in this analysis.

The FESR, Eq. (2.7), has some problem. i.e., there are the so-called unphysical regions coming from boson poles below the $\bar{p}p$ threshold. So, the contributions from unphysical regions of the first term of the right-hand side of Eq. (2.7) have to be calculated. These contributions can be estimated to be an order of 0.1% compared with the second term.¹⁾ Thus, it can easily be neglected.

Therefore, the FESR, the formula of $\sigma_{\text{tot}}^{(+)}$ (Eqs. (2.1) and (2.2)) and the $\rho^{(+)}$ ratio (Eq. (2.9)) are our starting points. Armed with the FESR, we express high-energy parameters $c_0, c_1, c_2, \beta_{P'}$ in terms of the integral of total cross sections up to N . Using this FESR as a constraint for $\beta_{P'} = \beta_{P'}(c_0, c_1, c_2)$, there are four independent parameters including $F^{(+)}(0)$. We then search for the simultaneous best fit to the data points of $\sigma_{\text{tot}}^{(+)}(k)$ and $\rho^{(+)}(k)$ for $70\text{GeV} \leq k \leq P_{\text{large}}$ corresponding to the SPS energy ($P_{\text{large}} \simeq 0.43 \times 10^6 \text{GeV}$ ($\sqrt{s} = 0.9\text{TeV}$)), to determine the values of c_0, c_1, c_2 and $F^{(+)}(0)$ giving the least χ^2 . We thus predict the σ_{tot} and $\rho^{(+)}$ in the Tevatron energy region ($\sqrt{s} = 1.8\text{TeV}$).

§3. Predictions for $\sigma_{\text{tot}}^{(+)}$ and $\rho^{(+)}$ at $\sqrt{s} = 1.8\text{TeV}$

Using the data up to $\sqrt{s} = 0.9\text{TeV}$ (SPS), we predict $\sigma_{\text{tot}}^{(+)}$ and $\rho^{(+)}$ at the Tevatron energy ($\sqrt{s} = 1.8\text{TeV}$).

Analysis 1: As was explained in the general approach (§2), both $\sigma_{\text{tot}}^{(+)}$ and $\text{Re } F^{(+)}$ data in $70\text{GeV} < k < P_{\text{large}} = 4.3 \times 10^5 \text{GeV}$ ($\sqrt{s} = 0.9\text{TeV}$) are fitted simultaneously through the formula of $\sigma_{\text{tot}}^{(+)}$ (Eqs. (2.1) and (2.2)) and the $\rho^{(+)}$ ratio (Eq. (2.9)) with the FESR (Eq. (2.7)) as a constraint.

The $\sigma_{\text{tot}}^{(+)}(k)$ data points are obtained by averaging $\sigma_{\text{tot}}^{\bar{p}p}$ and σ_{tot}^{pp} data points¹⁴⁾ when they are listed at the same value of k . For the details of data treatment of $\sigma_{\text{tot}}^{(+)}$ and $\text{Re } F^{(+)}$, see ref. 1). The FESR gives us

$$8.87 = c_0 + 2.04c_1 + 4.26c_2 + 0.367\beta_{P'} \quad (3.1)$$

(Eq. (12) of ref. 1)), where we use the central value of $\frac{1}{4\pi} \int_0^{\bar{N}} k^2 \sigma_{\text{tot}}^{(+)}(k) = 3403 \pm 20 \text{GeV}^*$ for $\bar{N} = 10 \text{GeV}$ in Eq. (2.7).

The result of the fit is shown in Fig. 1. The values of parameters and resulting χ^2 are given in Tables I and II, respectively.

Table I. The values of parameters in the best fit to the data up to SPS energy ($\sqrt{s} = 0.9 \text{TeV}$) in the analysis 1 (fit to the data in $70 \text{GeV} < k < P_{\text{large}} = 4.3 \times 10^5 \text{GeV}$). The error estimations are done as follows: The c_2 is fixed with a value deviated a little from the best-fit value, and then the χ^2 -fit is done by three parameters c_0 , c_1 and $F^{(+)}(0)$, where $\beta_{P'}$ is represented by the other parameters through FESR (Eq. (3.1)). When the resulting χ^2 is larger than the least χ^2 of the four-parameter fit by one, the corresponding value of c_2 gives one standard deviation. The higher and lower dot-dashed lines in Fig. 1 represent this deviation of c_2 . The errors of the other parameters are estimated through similar procedures.

	c_2	c_1	c_0	$\beta_{P'}$	$F^{(+)}(0)$
Analysis 1	0.0466 ± 0.0047	-0.161 ∓ 0.078	6.27 ± 0.33	7.45 ∓ 0.51	12.65 ± 5.66

Table II. The values of χ^2 for the fit to data in $70 \text{GeV} < k < P_{\text{large}} = 4.3 \times 10^5 \text{GeV}$ (Analysis 1): N_F and $N_\sigma(N_\rho)$ are the degree of freedom and the number of $\sigma_{\text{tot}}^{(+)}(\rho^{(+)})$ data points in the fitted energy region.

	χ^2/N_F	χ_σ^2/N_σ	χ_ρ^2/N_ρ
Analysis 1	8.1/20	5.7/17	2.4/8

In terms of the best-fit values of parameters in Table I the predictions at $\sqrt{s} = 1.8 \text{TeV}$ are obtained as

$$\sigma_{\text{tot}}^{(+)} = 75.9 \pm 1.0 \text{ mb}, \quad \rho^{(+)} = 0.136 \pm 0.005, \quad (3.2)$$

where the errors correspond to the one standard deviation of c_2 , since the $c_2 \log^2(\nu/M)$ -term in Eq. (2.2) is most relevant for predicting $\sigma_{\text{tot}}^{(+)}$ in high energy region. (See the caption in Table I.)

The equation (3.2) has to be compared with the experimental values at $\sqrt{s} = 1.8 \text{TeV}$;

$$\begin{aligned} \sigma_{\text{tot}}^{\bar{p}p}(E811) &= 71.71 \pm 2.02 \text{ mb}, \\ \sigma_{\text{tot}}^{\bar{p}p}(E710) &= 72.8 \pm 3.1 \text{ mb}, \\ \sigma_{\text{tot}}^{\bar{p}p}(CDF) &= 80.03 \pm 2.24 \text{ mb}, \end{aligned} \quad (3.3)$$

where we note that the difference between $\sigma_{\text{tot}}^{\bar{p}p}$ and $\sigma_{\text{tot}}^{(+)}$ is negligible at the relevant energy. It is worthwhile to notice that only the data of E710⁷⁾ is consistent with the prediction, Eq. (3.2) in the one standard deviation ($72.8 + 3.1 = 75.9$).

If one tolerates two standard deviations, both CDF⁹⁾ ($80.03 - 2.24 \times 2 = 75.55$) and E811⁸⁾ ($71.71 + 2.02 \times 2 = 75.75$) are consistent with the predictions Eq. (3.2).

*) This value is obtained by numerically integrating the experimental $k^2 \sigma_{\text{tot}}^{(+)} = k^2 (\sigma_{\text{tot}}^{\bar{p}p} + \sigma_{\text{tot}}^{pp})/2$. See, ref. 1) for details.

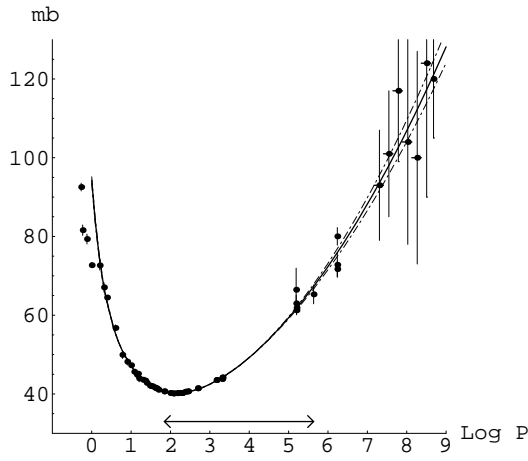
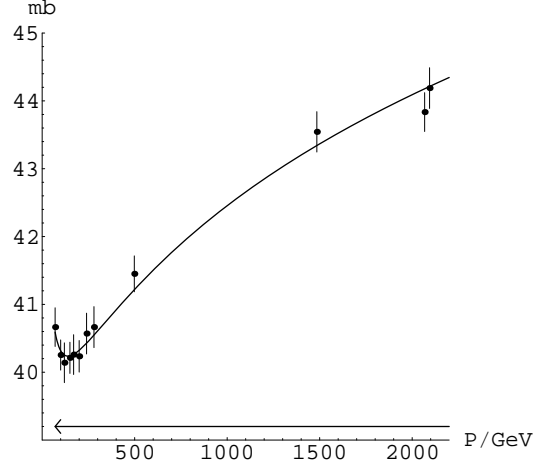
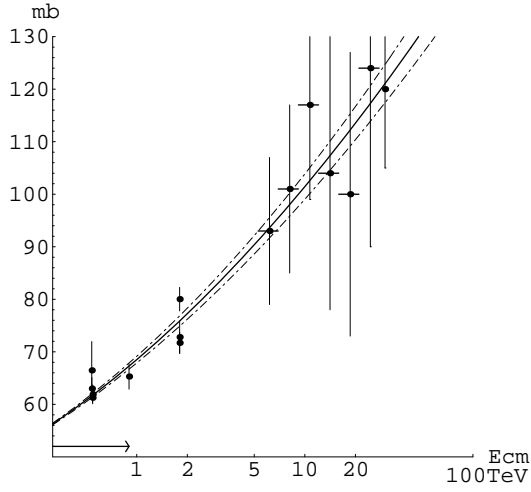
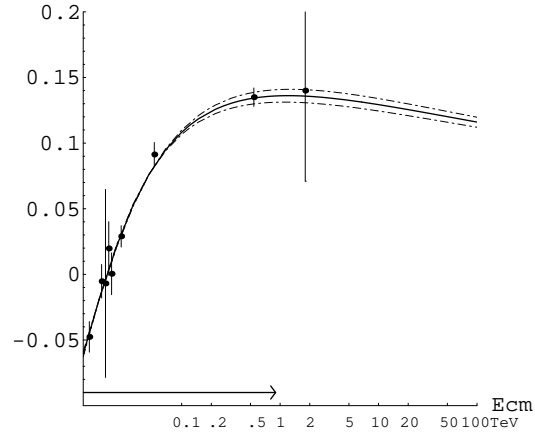
(a) $\sigma_{\text{tot}}^{(+)}$: All region(b) $\sigma_{\text{tot}}^{(+)}$: Low energy region(c) $\sigma_{\text{tot}}^{(+)}$: High energy region(d) $\rho^{(+)}$

Fig. 1. Predictions for $\sigma^{(+)}$ and $\rho^{(+)}$ in terms of the Analysis 1. The fit is done for the data up to SPS energy, in the region $70\text{GeV} \leq k \leq 4.3 \times 10^5\text{GeV}$ ($11.5\text{GeV} \leq \sqrt{s} \leq 0.9\text{TeV}$) which is shown by the arrow. Total cross section $\sigma_{\text{tot}}^{(+)}$ in (a) all energy region, versus $\log_{10} P_{\text{lab}}/\text{GeV}$, (b) low energy region (up to ISR energy), versus $P_{\text{lab}}/\text{GeV}$ and (c) high energy (Tevatron-collider, LHC and cosmic-ray energy) region, versus center of mass energy E_{cm} in TeV unit. (d) gives the $\rho^{(+)} (= \text{Re } F^{(+)} / \text{Im } F^{(+)})$ in high energy region, versus E_{cm} in terms of TeV. The thin dot-dashed lines represent the one standard deviation of c_2 . (See the caption in Table I.) The corresponding values of parameters are $(c_2, c_1, c_0, \beta_{P'}, F^{(+)}(0)) = (0.0466 \pm 0.0047, -0.161 \mp 0.077, 6.27 \pm 0.31, 7.45 \mp 0.48, 12.65 \pm 0.69)$.

So we can conclude that E710 is preferable but we can exclude neither CDF nor E811 results.

The predictions at LHC energy ($\sqrt{s} = 14\text{TeV}$) in terms of the best fit values of high-energy parameters in Table I are

$$\sigma_{\text{tot}}^{pp} = 107.2 \pm 2.8 \text{ mb}, \quad \rho^{pp} = 0.128 \pm 0.005, \quad (3.4)$$

where the errors correspond to one standard deviation of c_2 . We should note that Eq. (3.4) is consistent with the recent prediction by Block and Halzen,³⁾ $\sigma_{\text{tot}}^{pp} = 107.3 \pm 1.2 \text{ mb}$, $\rho^{pp} = 0.132 \pm 0.001$.

An interesting observation: We can make the following interesting observation. We fitted the data for $\sigma_{\text{tot}}^{(+)}$ and $\rho^{(+)}$ above 70GeV, as is shown by the arrow in the Fig. 1(a), Fig. 1(d) to predict higher-energy data. It is interesting to observe that the prediction of $\sigma_{\text{tot}}^{(+)}$ are also in good agreement with experiments, even below 70GeV. The reason is as follows: The requirement of FESR, Eq. (2.7) is nearly equal to require that the theoretical value of $\sigma_{\text{tot}}^{(+)}$ is nearly equal to the experimental value at the upper limit of the integral $N = 10\text{GeV}$ since higher side of the integral is enhanced because of k^2 in the integral.

Because of this observation, we can apply the same formula to fit the data in the lower energy region than in the analysis 1.

Analysis 2: Data in $10\text{GeV} < k < P_{\text{large}} = 4.3 \times 10^5 \text{GeV}$ ($4.54\text{GeV} < \sqrt{s} < 0.9\text{TeV}$) are fitted through the same formula in the analysis 1. Additionally 15(2) data points are included in $\sigma_{\text{tot}}^{(+)}$ ($Re F^{(+)}$).

The result of the fit is shown in Fig. 2. The values of parameters and resulting χ^2 are given in Tables III and IV, respectively.

Table III. The values of parameters in the best fit to the data up to the SPS energy ($\sqrt{s} = 0.9\text{TeV}$) in the analysis 2(fit to the data in $10\text{GeV} < k < P_{\text{large}} = 4.3 \times 10^5 \text{GeV}$). We obtain smaller error of $F^{(+)}(0)$ than in analysis 1(Table I), since, as is seen in Eq. (2.9), $F^{(+)}(0)$ has sizable effects only in the low energy region. For errors, see the caption in Table I.

	c_2	c_1	c_0	$\beta_{P'}$	$F^{(+)}(0)$
Analysis 2	0.0479 ± 0.0037	-0.186 ∓ 0.057	6.38 ± 0.22	7.26 ∓ 0.33	10.19 ± 1.72

Table IV. The values of χ^2 for the fit to data in $10\text{GeV} < k < P_{\text{large}} = 4.3 \times 10^5 \text{GeV}$ (Analysis 2). For N_F and $N_\sigma(N_\rho)$, see the caption in Table. II.

	χ^2/N_F	χ_σ^2/N_σ	χ_ρ^2/N_ρ
Analysis 2	14.1/37	8.8/32	5.3/10

The predictions at LHC energy ($\sqrt{s} = 14\text{TeV}$) in terms of the best fit values of high-energy parameters in Table III are

$$\sigma_{\text{tot}}^{pp} = 107.8 \pm 2.4 \text{ mb}, \quad \rho^{pp} = 0.129 \pm 0.004, \quad (3.5)$$

where the errors correspond to the one standard deviation of c_2 . Essentially the same prediction are obtained as Eq. (3.4) of the analysis 1, although the errors are slightly smaller. Our result is stable independently of the choices of the fitting energy range.

§4. Concluding remarks

In §3, we have investigated a possibility to resolve the discrepancy between E710, E811 and CDF, using the experimental data of $\sigma_{\text{tot}}^{(+)}$ and $\rho^{(+)}$ up to the SPS experiments ($\sqrt{s} = 0.9\text{TeV}$).

We came to the conclusion that only the data of E710 is consistent with the prediction, Eq. (3.2) in the one standard deviation although we can exclude neither CDF nor E811 results in the two standard deviations. In our previous paper, ref. 1) we concluded that the precise measurements of σ_{tot}^{pp} in the coming LHC measurements will resolve this discrepancy at $\sqrt{s} = 1.8\text{TeV}$. It would still be worthwhile, however, to fix this problem in the CDF and D0 experiments, since these values play an important role to search for $\sigma_{\text{tot}}^{(+)}$ and $\rho^{(+)}$ in the higher energy regions.

Appendix A

—— *Reanalysis of our predictions at the LHC ($\sqrt{s}=1.8\text{TeV}$) with $F^{(+)}(0)$ parameter* ——

In our previous work,¹⁾ we exploited the experimental data $\sigma_{\text{tot}}^{(+)}$ and $\rho^{(+)}$ above $P_{\text{lab}}=70\text{GeV}$ up to Tevatron energy ($\sqrt{s} = 1.8\text{TeV}$) to predict $\sigma_{\text{tot}}^{(+)}$ and $\rho^{(+)}$ in the LHC region, based on Eq. (2.8) of $\rho^{(+)}$, not by Eq. (2.9). Although the effect of the parameter $F^{(+)}(0)$ in the new formula (Eq. (2.9)) is not large in the high energy region, we show the results of the analyses based on Eq. (2.9) here for completeness.

Corresponding to ref. 1) two independent analyses are done: one includes the E710/E811 data at $\sqrt{s}=1.8\text{TeV}$ denoted as fit 2 in ref. 1), and the other includes the CDF datum of $\sigma_{\text{tot}}^{(+)}$ at the same energy denoted as fit 3 in ref. 1). The results of the simultaneous fit to $\sigma_{\text{tot}}^{(+)}$ and $\rho^{(+)}$ are compared with the previous results¹⁾ in Fig. 3. The fit to $\rho^{(+)}$ is slightly improved in the lower energy region, while the result of $\sigma_{\text{tot}}^{(+)}$ is almost the same as the previous one. The obtained values of parameters and the resulting χ^2 are given in Table V and Table VI, respectively.

Table V. The best-fit values of parameters in the fit 2 (fit up to Tevatron-collider energy including E710/811 data) and fit 3 (including CDF datum). The errors here correspond to the one standard deviation of c_2 . (See the caption in Table I.)

	c_2	c_1	c_0	$\beta_{P'}$	$F^{(+)}(0)$
fit 2	0.0424 ± 0.0041	-0.099 ∓ 0.069	6.04 ± 0.28	7.61 ∓ 1.55	12.48 ± 0.73
fit 3	0.0496 ± 0.0043	-0.205 ∓ 0.072	6.44 ± 0.29	7.20 ∓ 0.81	12.78 ± 0.72

The fit to $\rho^{(+)}$ in the lower energy region is improved in comparison with the previous result, as can be seen in Fig. 3. Correspondingly much smaller χ_ρ^2 is obtained in Table VI, which is compared with the previous values, $\chi_\rho^2=8.4(6.9)$ for fit 2(3).¹⁾

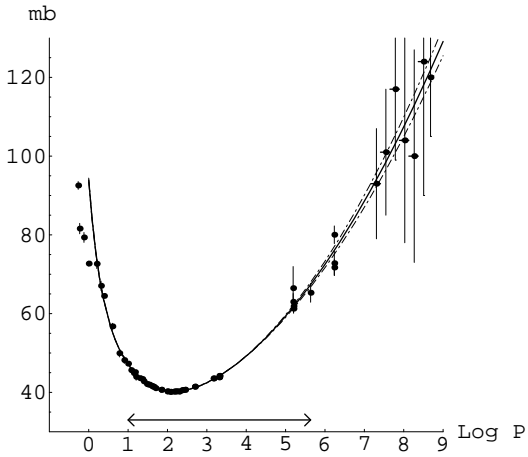
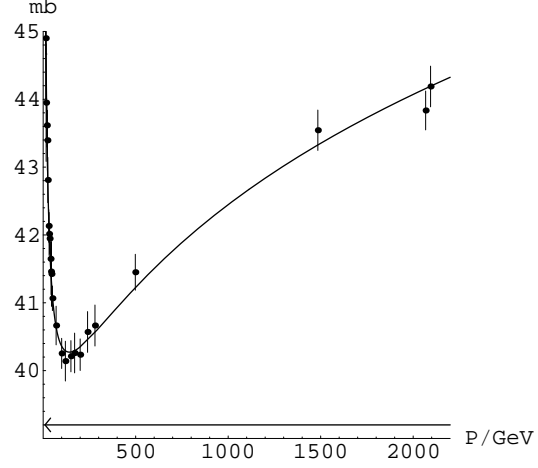
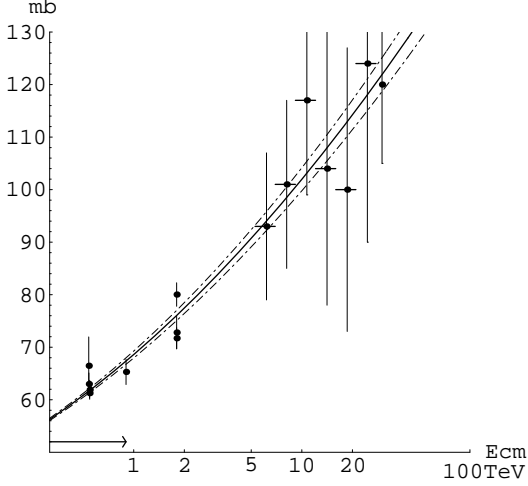
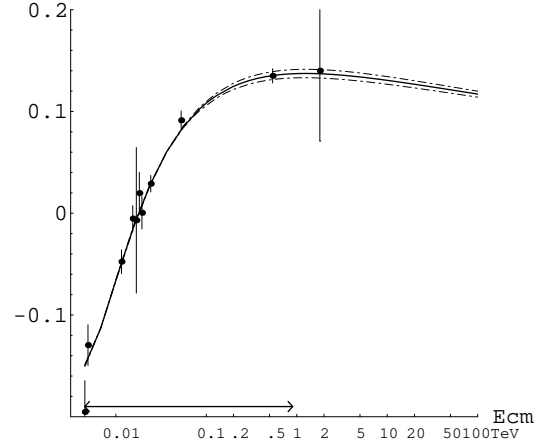
(a) $\sigma_{\text{tot}}^{(+)}$: All region(b) $\sigma_{\text{tot}}^{(+)}$: Low energy region(c) $\sigma_{\text{tot}}^{(+)}$: High energy region(d) $\rho^{(+)}$

Fig. 2. Predictions for $\sigma^{(+)}$ and $\rho^{(+)}$ in terms of the Analysis 2. The fit is done for the data up to SPS energy, in the region $10\text{GeV} \leq k \leq 4.3 \times 10^5 \text{GeV}$ ($4.54\text{GeV} \leq \sqrt{s} \leq 0.9\text{TeV}$) which is shown by the arrow. For each figure, see the caption in Fig. 1. The thin dot-dashed lines represent the one standard deviation of c_2 . (See the caption in Table I.) The corresponding values of parameters are $(c_2, c_1, c_0, \beta_{P'}, F^{(+)}(0)) = (0.0479 \pm 0.0037, -0.186 \mp 0.056, 6.38 \pm 0.21, 7.26 \mp 0.31, 10.19 \pm 0.31)$.

Table VI. The values of χ^2 for the fit 2 and fit 3. N_F and $N_\sigma(N_\rho)$ are the degree of freedom and the number of $\sigma_{\text{tot}}^{(+)}(\rho^{(+)})$ data points in the fitted energy region.

	χ^2/N_F	χ_σ^2/N_σ	χ_ρ^2/N_ρ
fit 2	11.6/22	7.9/18	3.7/9
fit 3	10.9/22	8.7/18	2.1/9

Predicted values of $\sigma_{\text{tot}}^{(+)}$ and $\rho^{(+)}$ at LHC energy ($\sqrt{s}=14\text{TeV}$) and at cosmic-ray energy ($P_{\text{lab}}=5 \times 10^{20}\text{eV}$) are given in Table VII.

Table VII. The predictions of $\sigma_{\text{tot}}^{(+)}$ and $\rho^{(+)}$ at the LHC energy $\sqrt{s} = E_{\text{cm}} = 14\text{TeV}$ ($P_{\text{lab}}=1.04 \times 10^8\text{GeV}$), and at a very high energy $P_{\text{lab}} = 5 \cdot 10^{20}\text{eV}$ ($\sqrt{s}=E_{\text{cm}}=967\text{TeV}$) in the cosmic-ray region. The errors correspond to one standard deviation of c_2 .

	$\sigma_{\text{tot}}^{(+)}(\sqrt{s}=14\text{TeV})$	$\rho^{(+)}(\sqrt{s}=14\text{TeV})$	$\sigma_{\text{tot}}^{(+)}(P_{\text{lab}}=5 \cdot 10^{20}\text{eV})$	$\rho^{(+)}(P_{\text{lab}}=5 \cdot 10^{20}\text{eV})$
fit 2	$104.2 \pm 2.3\text{mb}$	0.123 ± 0.004	$191 \pm 8\text{mb}$	0.100 ± 0.003
fit 3	$109.3 \pm 2.4\text{mb}$	0.130 ± 0.004	$206 \pm 8\text{mb}$	0.105 ± 0.003

The predictions combining the two results in Table VII are

$$\begin{aligned}
 \sigma_{\text{tot}}^{\bar{p}p} &= 106.8 \pm 5.1_{\text{syst}} \pm 2.4_{\text{stat}} \text{ mb}, \quad \rho^{\bar{p}p} = 0.127 \pm 0.007_{\text{syst}} \pm 0.004_{\text{stat}} \\
 \sigma_{\text{tot}}^{pp} &= 198 \pm 16_{\text{syst}} \pm 8_{\text{stat}} \text{ mb}, \quad \rho^{pp} = 0.103 \pm 0.004_{\text{syst}} \pm 0.003_{\text{stat}}
 \end{aligned} \tag{A.1}$$

at the LHC energy ($\sqrt{s} = E_{\text{cm}} = 14\text{TeV}$) and the cosmic-ray energy ($P_{\text{lab}} = 5 \times 10^{20}\text{eV}$), respectively. The above results are almost the same as the previous ones, Eq. (13) of ref. 1). Here we obtain fairly large systematic uncertainty again coming from the data treatment at the Tevatron-energy.

References

- 1) K. Igi and M. Ishida, Phys. Lett. B **622** (2005), 286
- 2) M. M. Block and F. Halzen, Phys. Rev. D **72** (2005), 036006: Erratum 039902.
- 3) M. M. Block and F. Halzen, hep-ph/0510238.
- 4) M. Honda et al. (Akeno Collab.), Phys. Rev. Lett. **70** (1993), 525.
- 5) R. M. Baltrusaitis et al. (Fly's Eye Collab.), Phys. Rev. Lett. **52** (1984), 1380
- 6) M. M. Block, F. Halzen and T. Stanev, Phys. Rev. D **62** (2000), 077501.
- 7) N. A. Amos, et al., E-710 Collaboration, Phys. Rev. Lett. **68** (1992), 2433.
- 8) C. Avila, et al., E-811 Collaboration, Phys. Lett. B **445** (1999), 419.
- 9) F. Abe, et al., CDF Collaboration, Phys. Rev. D **50** (1994), 5550.
- 10) K. Igi and M. Ishida, Phys. Rev. D **66** (2002), 034023.
- 11) K. Igi and S. Matsuda, Phys. Rev. Lett. **18** (1967), 625.
- 12) R. Dolen, D. Horn and C. Schmid, Phys. Rev. **166** (1968), 1768.
- 13) M. M. Block and R. N. Cahn, Rev. Mod. Phys. **57** (1985), 563.
- 14) Particle Data Group, S. Eidelman et al., Phys. Lett. B **592** (2004), 313.

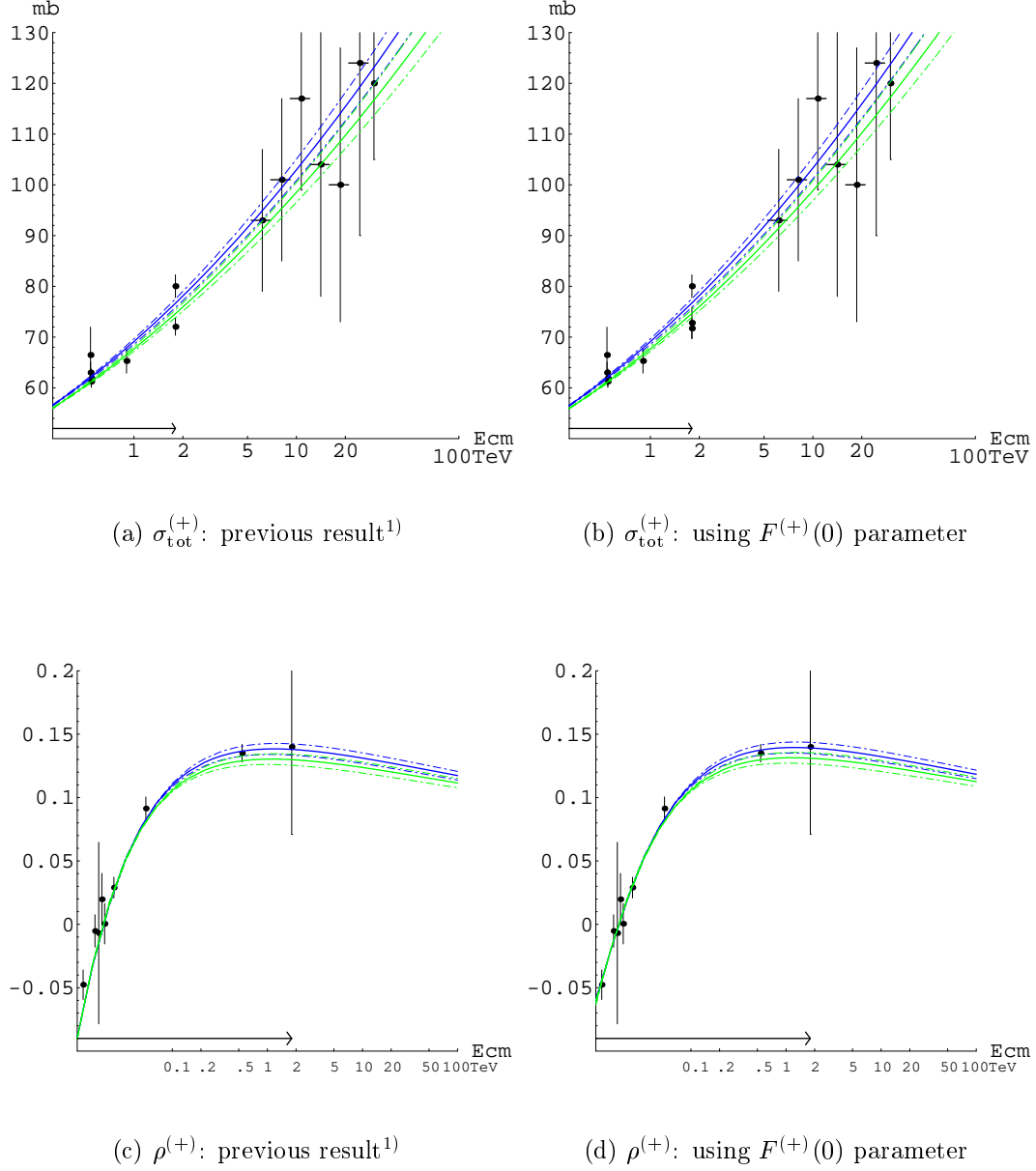


Fig. 3. Predictions for $\sigma^{(+)}$ and $\rho^{(+)}$ compared with the previous results: The new results using $F^{(+)}(0)$ parameter are shown by right figures, (b) and (d), respectively, which are compared with the left figures, (a) and (c), of the previous analyses.¹⁾ Predictions in terms of the fit 2(3) are shown by green(blue) lines, and the thin dot-dashed lines represent the one standard deviation of c_2 . (See the caption in Table I.) The corresponding values of parameters are given in Table V.